



## Krakatoa lives: The effect of volcanic eruptions on ocean heat content and thermal expansion

P. J. Gleckler,<sup>1</sup> K. AchutaRao,<sup>1</sup> J. M. Gregory,<sup>2</sup> B. D. Santer,<sup>1</sup> K. E. Taylor,<sup>1</sup> and T. M. L. Wigley<sup>3</sup>

Received 1 May 2006; revised 22 June 2006; accepted 14 July 2006; published 1 September 2006.

[1] A suite of climate model experiments indicates that 20th Century increases in ocean heat content and sea-level (via thermal expansion) were substantially reduced by the 1883 eruption of Krakatoa. The volcanically-induced cooling of the ocean surface is subducted into deeper ocean layers, where it persists for decades. Temporary reductions in ocean heat content associated with the comparable eruptions of El Chichón (1982) and Pinatubo (1991) were much shorter lived because they occurred relative to a non-stationary background of large, anthropogenically-forced ocean warming. Our results suggest that inclusion of the effects of Krakatoa (and perhaps even earlier eruptions) is important for reliable simulation of 20th century ocean heat uptake and thermal expansion. Inter-model differences in the oceanic thermal response to Krakatoa are large and arise from differences in external forcing, model physics, and experimental design. Systematic experimentation is required to quantify the relative importance of these factors. The next generation of historical forcing experiments may require more careful treatment of pre-industrial volcanic aerosol loadings.  
**Citation:** Gleckler, P. J., K. AchutaRao, J. M. Gregory, B. D. Santer, K. E. Taylor, and T. M. L. Wigley (2006), Krakatoa lives: The effect of volcanic eruptions on ocean heat content and thermal expansion, *Geophys. Res. Lett.*, 33, L17702, doi:10.1029/2006GL026771.

### 1. Introduction

[2] There is observational evidence that global ocean temperatures have increased over the last 50 years [e.g., *Levitus et al.*, 2005]. Global mean sea level has risen as a result of thermal expansion of the warming oceans, with additional sea level rise from glacier and ice sheet melt [e.g., *Church et al.*, 2001]. Using results from recent climate modeling experiments, this study examines the impact of volcanic eruptions on ocean warming and the associated thermal expansion.

[3] Experiments with coupled Ocean-Atmosphere General Circulation Models (OAGCMs) now routinely include a range of time-varying natural and anthropogenic external forcings. Models driven by estimates of external forcings have been able to reproduce the linear trend component of

the late 20th Century observed ocean warming and attribute it to increasing greenhouse gas concentrations [e.g., *Barnett et al.*, 2005; *Levitus et al.*, 2001].

[4] *Church et al.* [2005] compared results from OAGCM simulations with observed estimates of global ocean heat content (OHC) and global mean sea level (GMSL). They showed that the eruption of Pinatubo in 1991 led to rapid reductions in OHC and GMSL, with recovery taking up to a decade. More recently, *Gleckler et al.* [2006] (hereinafter referred to as G06) examined the OHC and GMSL changes in a new suite of climate model experiments. The G06 study suggested that volcanic eruptions could have more prominent and longer lasting effects, particularly the eruption of Krakatoa in 1883. The results of G06 clearly distinguish models that included volcanic forcing from those that did not, suggesting that historical eruptions have been sufficient to offset a large fraction of the OHC and GMSL increases caused by anthropogenic influences over the 20th Century. In this study, we explore the suite of model experiments used in G06 in more detail. We focus on the individual simulations that included volcanic forcing, and their global OHC and GMSL recovery after Krakatoa and subsequent eruptions.

### 2. Methods

[5] A new suite of OAGCM simulations has recently been performed by the climate modeling community. We focus on the “Climate of the 20th Century” historical forcing experiment (20c3m), in which each model was run with a variety of external climate forcings, such as changes in well-mixed greenhouse gases (GHGs), sulphate aerosol concentrations, solar irradiance, and volcanic aerosol loadings. Since the development of many of these historical forcings is still an active research topic, standard forcing data sets were not prescribed as part of the 20c3m experiment. Instead, the 20c3m runs represent each groups’ best effort to simulate 20th Century climate. The models used in this study and the external forcings applied to them are summarized in supplementary information of G06. *Stenchikov et al.* [2006] discuss how the different volcanic data sets were constructed.

[6] Our methods for calculating ocean heat content and thermal expansion, as detailed in the supplemental information of G06, have been demonstrated to be appropriate for global average calculations [e.g., *Gregory and Lowe*, 2000; *Russell et al.*, 2000; *Gregory et al.*, 2001]. Each of the 20c3m experiments examined here are spawned from some point of a control run forced with constant pre-industrial GHG concentrations. To remove the influence of climate drift (see below), we examine contemporaneous

<sup>1</sup>Program for Climate Model Diagnosis and Intercomparison, Lawrence Livermore National Laboratory, Livermore, California, USA.

<sup>2</sup>Department of Meteorology, University of Reading, Reading, UK.

<sup>3</sup>National Center for Atmospheric Research, Boulder, Colorado, USA.

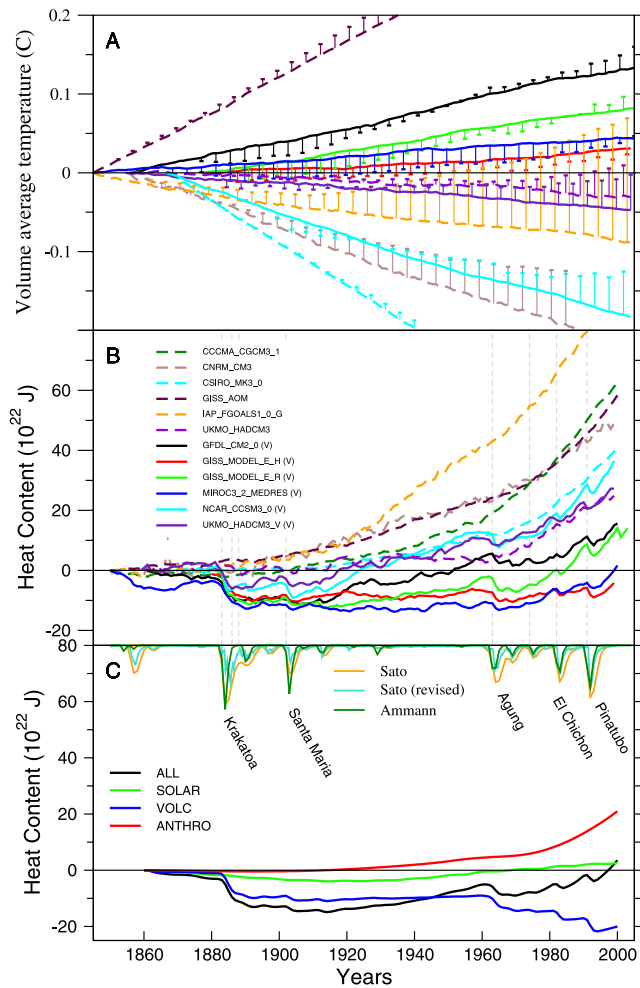


**Figure 1.** (a) Global ocean volume average temperature (degrees C). Coupled model departures from the 20c3m initial state are shown for each control run (lines) and contemporaneous departures of the 20c3m from the control runs (vertical bars). (b) 20c3m global ocean heat content ( $10^{22}$  Joules) departures from the contemporaneous portion of the control run. Vertical dashed lines indicate dates of major eruptions. Figures 1a and 1b show simulations with volcanic forcing (solid) and without (dashed). (c) Global ocean heat content ( $10^{22}$  Joules) from a simple climate model (MAGICC) driven by individual natural forcings (solar, volcanic), various anthropogenic forcings (ANTHRO), and combined natural and anthropogenic forcings (ALL). Three volcanic data sets (arbitrary scale) typify the forcings used in the 20c3m simulations examined.

departures of the 20c3m runs from their corresponding control runs.

### 3. Results

[7] Figure 1a shows control run and 20c3m temperature anomalies for the global ocean, expressed as departures from the initial state of the 20c3m run. Control runs are represented by lines (solid for those models including volcanic effects in their 20c3m runs, dashed for those without) while the 20c3m departures relative to these are shown as vertical bars. The quantity plotted in Figure 1a is

proportional to global OHC. The control runs show drifts (some positive, some negative) because they were not started from a steady state and it is not computationally feasible to “spin up” an OAGCM for the hundreds or even thousands of years required for complete equilibrium. These drifts are generally linear, suggesting small but persistent imbalances in the global ocean surface net heat budget. For many models the drift is noticeably larger than the corresponding 20c3m signals, because the drift penetrates into the abyssal ocean whereas the 20c3m signal is mostly contained in the top 500 meters. For most models, the drift in the top 500 meters is small compared to the 20c3m signal (not shown).

[8] The 20c3m OHC departures from the contemporaneous control runs are shown in Figure 1b. By the end of the 20th Century, the accumulated ocean heat uptake from the pre-industrial initial state ranges from  $-4$  to  $90 \times 10^{22}$  J (Figure 1b). Following the 1883 eruption of Krakatoa (augmented by the relatively small eruptions of Tarawera in 1886 and Bandai in 1888, see Figure 1c), there is a clear separation between the models that included volcanic forcing (V, solid lines) and those that did not (non-V, dashed lines). Volcanic aerosols scatter and absorb sunlight, reducing the total net air-sea heat flux, resulting in a cold sea surface temperature anomaly that is gradually subducted into deeper layers. As noted in G06, the ocean heat uptake at the end of the 20th Century is generally lower in the V simulations. NCAR-CCSM3 is an exception, with overall heat uptake that is greater than in one of the non-V models (UKMO-HADCM3). Note also that at year 2000 the OHC differences between the UKMO-HADCM3 V and non-V runs are comparatively small (see discussion section).

[9] Shortly after the Bandai eruption (1888), the OHC achieves minimum values in the V models (Figure 1b). In four of these models it is of order of  $-10 \times 10^{22}$  J, although the GFDL-CM2-0 and MIROC3-2-MEDRES models have pronounced negative OHC anomalies even before the Krakatoa eruption. Note that the cold anomaly at the time of Bandai is smaller in the NCAR-CCSM3 and UKMO-HADCM3-V models than in the other four V models.

[10] All V models show rapid reductions in OHC after the eruptions of Agung (1963), El Chichón (1982) and Pinatubo (1991). The duration of these reductions is much shorter than for Krakatoa. The reason for this discrepancy is that the late 20th Century eruptions occur relative to a non-stationary background of large, anthropogenically-forced changes in OHC. To illustrate this, we carried out simulations using the MAGICC upwelling-diffusion energy-balance model [Wigley and Raper, 2001], which has been shown to emulate accurately the results of OAGCMs on both century and sub-decadal [Wigley *et al.*, 2005] time scales. In the absence of positive forcings, the cumulative effect of volcanically-induced OHC decreases is more obvious, with the magnitude of the OHC decrease dependent on both the peak and integrated forcings of each eruption (Figure 1c). Inclusion of combined anthropogenic and natural effects in MAGICC (the ‘ALL’ case in Figure 1c) yields results that mimic the time evolution of OHC changes in the coupled model runs with V forcing (Figure 1b). The individually forced MAGICC results shown here are qualitatively consistent with comparable forcing experiments performed with the GFDL OAGCM

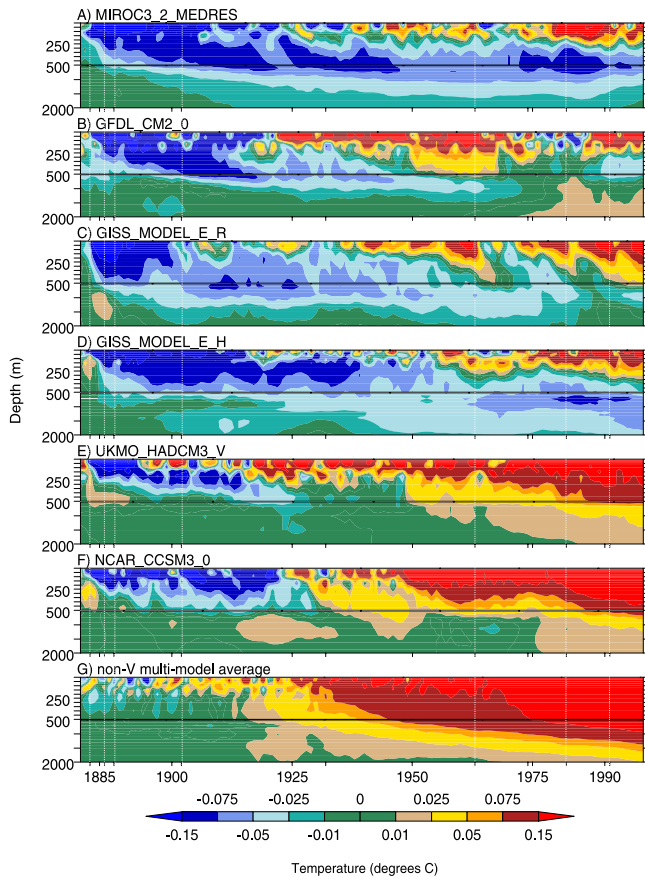


**Figure 2.** Changes in annual-mean global ocean temperature (degrees C) as a function of depth (m) in coupled model experiments with (a–f) combined anthropogenic and volcanic forcing and (g) in experiments with anthropogenic forcing only. Anomalies were defined as described in Figure 1b. The non-V model average is based on the six OAGCMs without V forcing. Vertical dashed lines indicate dates of major eruptions.

[Delworth *et al.*, 2005a, 2005b], which illustrate the relative impact of natural (solar and volcanic) and anthropogenic forcing on OHC.

[11] Figure 2 shows the penetration of the Krakatoa-induced cooling anomaly into deeper ocean layers. The six V simulations (Figures 2a–2f) show qualitative similarities in their responses to Krakatoa, although the cold anomalies in the UKMO-HADCM3-V and NCAR-CCSM3-0 do not penetrate as deeply and have shorter-lived cooling signatures. This distinction is important, and we refer subsequently to MIROC3-2-MEDRES, GFDL-CM2-0, GISS-E-R, GISS-E-H as the cool V models ( $V_{COOL}$ ) and to UKMO-HADCM3-V and NCAR-CCSM3-0 as the warm V models ( $V_{WARM}$ ). At the end of the 20th Century, the ocean heat uptake of the  $V_{COOL}$  models is less than for the  $V_{WARM}$  models. In the simulations that exclude V forcing (Figure 2g), the surface warming begins sooner and mixes deeper than in any of the V models.

[12] By the 1930s, the surface is warming in response to anthropogenic forcing in all models, and the effect of Krakatoa at depth is no longer evident in the  $V_{WARM}$  models. In the  $V_{COOL}$  models, the Krakatoa anomaly is decoupled

from the surface warming and lingers below it, in some cases until the end of the 20th Century (Figures 2a–2d). While late 20th Century eruptions are partly responsible for the continued sub-surface cooling, only the Krakatoa signal has penetrated sufficiently deep to be isolated from the mixed layer and the encroaching warming from above.

[13] Immediately following the Krakatoa-Tarawera-Bandai eruptions of the 1880s, the 0–1500 meter OHC cold anomaly in the  $V_{COOL}$  models is noticeably larger than the  $V_{WARM}$  models (Figure 3a). There is little evidence of an OHC trend until the 1920s, at which point the  $V_{WARM}$  models and GFDL-CM2-0 begin warming. Following Agung (1963), the  $V_{WARM}$  models continue warming unabated, whereas there is still little heat uptake in 3 of the 4  $V_{COOL}$  models. The impact of Agung is largest on GFDL-CM2-0 simulation, interrupting its steady warming and reducing its OHC to within the range of the other 3  $V_{COOL}$  models by 2000. In the upper 0–500 meters (Figure 3b) all V models begin recovery almost immediately following Krakatoa and thereafter exhibit a steady warming. The real difference is below 500 meters (Figure 3c), where the Krakatoa signal in the  $V_{COOL}$  models gradually penetrates over many decades. There is no evidence of this in the  $V_{WARM}$  models.

[14] Sea-level height depends on the column-integrated density, and therefore responds to temperature and salinity changes. Averaged globally, thermal expansion is the dominant contribution to overall sea level rise [Gregory and Lowe, 2000]. Since the models considered have no land ice melt contributions, their sea-level changes arise solely from thermal expansion. Global OHC and expansion time series

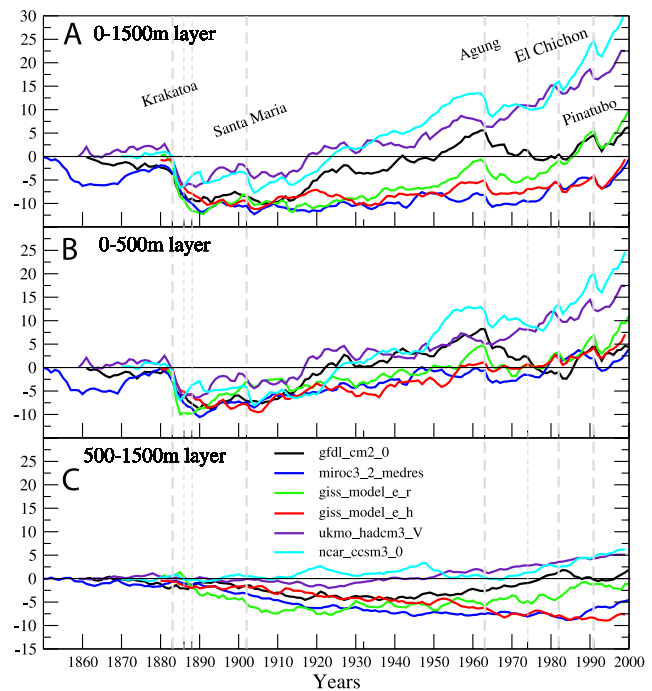


**Figure 3.** Changes in annual-mean global ocean heat content ( $10^{22}$  Joules) in coupled model simulations that include V forcing. Results are depth-integrated for three ocean layers: (a) 0–1500 meters; (b) 0–500 meters; and (c) 500–1500 meters. For anomaly definition, see Figure 1. Vertical dashed lines indicate dates of major eruptions.



**Table 1.** Changes in Simulated and Observed Ocean Heat Content and Thermal Expansion for the 0–3000 Meter Layer of the Global Ocean<sup>a</sup>

Model ID	V	OHC Trend 1955–1998, 10 <sup>22</sup> J/year	GMSL Trend 1955–1998, mm/yr	GMSL Change 1880–1998, mm
GFDL-CM2.0	Yes	0.06	−0.08	15.0
GISS-EH	Yes	0.00	0.07	0.7
GISS-ER	Yes	0.28	0.35	16.5
MIROC3.2-MED	Yes	0.16	0.21	3.3
NCAR-CCSM3	Yes	0.44	0.48	37.2
UKMO-HadCM3-V	Yes	0.39	0.32	20.4
Observed estimate	-	0.33	0.40	-
CCCma-CGCM3.1	No	1.00	1.22	65.5
CNRM-CM3	No	0.67	0.81	56.8
CSIRO-mk3.0	No	0.71	0.68	37.7
GISS-AOM	No	0.72	0.88	57.0
IAP-FGOALS-1.0g	No	1.26	1.29	87.5
UKMO-HadCM3	No	0.52	0.72	20.9

<sup>a</sup>Trends in thermal expansion and heat content were calculated from pentadal running means. The first (last) pentadal mean was for the period 1955–1959 (1994–1998). Expansion changes are the difference between the 1993–1998 and 1883–1888 pentadal means. The observed heat content trend is an estimate from *Levitus et al.* [2005]. The observed thermal expansion trend was obtained from *Antonov et al.* [2005].

are highly correlated [*Russell et al.*, 2000], and thus the evolution of GMSL in these simulations (not shown) closely corresponds to Figure 1b.

[15] Simulated GMSL changes from 1880 to the end of the 20th Century are given in Table 1 for the 0–3000 meter layer of the global ocean. Consistent with our findings for OHC (Figure 1b), the expansion values in the V simulations are lower. Table 1 also provides recent estimates of the observed trends in heat content and thermal expansion over 1955–1998 [*Levitus et al.*, 2005; *Antonov et al.*, 2005]; although it should be noted that these values are affected by incomplete observational coverage [*AchutaRao et al.*, 2006]. For both heat content and expansion, trends in the non-V runs are substantially larger than the observed results. Observed trends are contained within the range of V model results. Similar conclusions can be drawn from the shorter post-Pinatubo period as examined by *Church et al.* [2005].

#### 4. Discussion and Implications

[16] We have compared the behavior of six coupled climate simulations that included the effects of volcanic eruptions with six that did not. The twelve models have differences in physics, resolution, initial conditions, ‘spin-up’ and coupling procedures, as well as the types of external forcings used. Our investigation therefore incorporates uncertainties in both the applied forcings and in the model responses to these forcings. We find that inclusion of volcanic forcing has a dramatic effect on simulated changes in ocean heat content and sea level over the 20th century, especially the eruption of Krakatoa in 1883. However, there are important discrepancies between these simulations, resulting from differences in ocean mixing efficiencies, assumed external forcing, and the experimental design (discussed below).

[17] Two of the six simulations (NCAR-CCSM3-0 and UKMO-HADCM3) examined had weaker responses to Krakatoa and subsequently exhibit substantially more 20th Century ocean heat uptake than the other four. NCAR-CCSM3-0 was the only one to be forced with the *Ammann et al.* [2003] estimate of volcano forcing, which in an integrated sense has much weaker Krakatoa forcing than

is evident in the two versions of the *Sato et al.* [1993] forcing applied by other groups (Figure 1c). At the time of the Tarawera eruption (1886), both versions of the *Sato et al.* aerosol optical depth data set have a substantial forcing from Krakatoa, while the *Ammann et al.* [2003] data set does not appear to include the effects of Tarawera and Bandai. Sensitivity experiments with the UKMO-HADCM3 model suggest that the magnitude of the initial drop in sea level scales nearly linearly with the eruption magnitude (*Gregory et al.*, 2006). However, as in our results, recovery from weaker forcing was somewhat more rapid and presumably due to differences in the anomaly penetration. Our results are clearly sensitive to the large uncertainties in historical reconstructions of volcanic aerosols [e.g., *Robock, 2000*; *Stenchikov et al.*, 2006] and anthropogenic aerosols. The latter have been shown to substantially reduce ocean heat uptake in the GFDL model used here [*Delworth et al.*, 2005b].

[18] One aspect of the experimental design may help to explain why the UKMO-HADCM3-V simulations has a less persistent ocean heat content signature of the Krakatoa eruption than the  $V_{COOL}$  models. The UKMO-HADCM3-V control run - unlike the others examined here - included forcing by a background volcanic aerosol (prescribed as the average volcanic forcing over the 20th century [see *Stott et al.*, 2000]). This forcing was meant to approximately account for the effects of pre-industrial eruptions on the mean climate state. It was turned off at the beginning of the 20th Century UKMO-HADCM3-V simulation, at which point the observed episodic volcanic forcing was imposed. In a linear system the long-term mean effects of episodic forcing should be similar to those of a mean background aerosol, so the heat uptake should on average not be affected too much by the time profile of volcanic forcing (compare the heat content of the UKMO-HADCM3 V and non-V simulations at 2000 in Figure 1b). Had UKMO-HADCM3-V been spawned from a control without background volcanic forcing, the ocean heat uptake at year 2000 would have been substantially less, and probably within the range of the  $V_{COOL}$  models. While some attention has been given to the importance of ocean initial conditions [e.g.,

Weaver et al., 2000], they clearly remain a challenge for accurate simulation of ocean heat uptake.

[19] An important issue beyond the scope of this study is the uncertainty associated with the parameterization of ocean mixing. The persistence of the Krakatoa anomaly is dependent on how deep it has penetrated within a few years of the eruption. Efforts to track the ‘Krakatoa anomaly’ in these simulations will require diagnosis of how and where mixing is occurring in multiple realizations of each model.

[20] In conclusion, our results imply that inclusion of volcanic forcing from Krakatoa and other eruptions is important for reliable simulation of historical increases in ocean heat content and the associated (via thermal expansion) sea level rise. The effects of eruptions before Krakatoa (which were not examined here) may also be important. These findings need to be studied further in the context of uncertainties associated with external forcings, model physics and experimental configuration. Systematic experimentation is needed to determine how best to include the effects of volcanic eruptions in historical forcing simulations, and whether to account for eruptions that pre-date the start of the simulation.

[21] **Acknowledgments.** Work at Lawrence Livermore National Laboratory (LLNL) was performed under the auspices of the U.S. Dept. of Energy, Environmental Sciences Division, contract W-7405-ENG-48. TMLW was supported by NOAA (Office of Climate Programs) under grant NA87GP0105 and by the U.S. Dept. of Energy under grant DE-FG02-98ER62601. NCAR is supported by the National Science Foundation. Work at the Hadley Centre was supported by the UK Department for Environment, Food and Rural Affairs under contract PECD 7/12/37 and by the Government Meteorological Research and Development Programme. The authors acknowledge the international modeling groups for providing their data for analysis, the JSC/CLIVAR Working Group on Coupled Modelling (WGCM) and their Coupled Model Intercomparison Project (CMIP) and Climate Simulation Panel for organizing the model data analysis activity, and the IPCC WG1 TSU for technical support. The IPCC Data Archive at Lawrence Livermore National Laboratory is supported by the Office of Science, U.S. Department of Energy.

## References

- AchutaRao, K. M., B. D. Santer, P. J. Gleckler, K. E. Taylor, D. W. Pierce, T. P. Barnett, and T. M. L. Wigley (2006), Variability of ocean heat uptake: Reconciling observations and models, *J. Geophys. Res.*, *111*, C05019, doi:10.1029/2005JC003136.
- Ammann, C. M., G. A. Meehl, W. M. Washington, and C. S. Zender (2003), A monthly and latitudinally varying volcanic forcing data set in simulations of 20th century climate, *Geophys. Res. Lett.*, *30*(12), 1657, doi:10.1029/2003GL016875.
- Antonov, J. I., S. Levitus, and T. P. Boyer (2005), Thermosteric sea level rise, 1955–2003, *Geophys. Res. Lett.*, *32*, L12602, doi:10.1029/2005GL023112.
- Barnett, T. P., et al. (2005), Penetration of human-induced warming into the World’s oceans, *Science*, *309*, 284–287, doi:10.1126/science.1112418.
- Church, J. A., et al. (2001), Changes in sea level, in *Climate Change 2001: The Scientific Basis: Contribution of Working Group I to the Third Assessment Report of the Intergovernmental Panel on Climate Change*, edited by J. T. Houghton et al., pp. 639–694, Cambridge Univ. Press, New York.
- Church, J. A., N. J. White, and J. M. Arblaster (2005), Significant decadal-scale impact of volcanic eruptions on sea level and ocean heat content, *Nature*, *438*, 74–77, doi:10.1038/nature04237.
- Delworth, T. L., et al. (2005a), GFDL’s CM2 global coupled climate models: Part 1: Formulation and simulation characteristics, *J. Clim.*, *19*(5), 643–674.
- Delworth, T. L., V. Ramaswamy, and G. L. Stenchikov (2005b), The impact of aerosols on simulated ocean temperature and heat content in the 20th century, *Geophys. Res. Lett.*, *32*, L24709, doi:10.1029/2005GL024457.
- Gleckler, P. J., et al. (2006), Krakatoa’s signature persists in the ocean, *Nature*, *439*, 675, doi:10.1038/439675.
- Gregory, J. M., and J. A. Lowe (2000), Predictions of global and regional sea-level rise using AOGCMs with and without flux adjustment, *Geophys. Res. Lett.*, *27*, 3069–3072.
- Gregory, J. M., et al. (2001), Comparison of results from several AOGCMs for global and regional sea-level change 1900–2100, *Clim. Dyn.*, *18*, 225–240, doi:10.1007/s003820100180.
- Gregory, J. M., J. A. Lowe, and S. F. B. Tett (2006), Simulated global mean sea-level changes over the last half-millennium, *J. Clim.*, in press.
- Levitus, S., J. I. Antonov, J. L. Wang, T. L. Delworth, K. W. Dixon, and A. J. Broccoli (2001), Anthropogenic warming of the Earth’s climate system, *Science*, *292*, 267–270.
- Levitus, S., J. Antonov, and T. Boyer (2005), Warming of the world ocean, 1955–2003, *Geophys. Res. Lett.*, *32*, L02604, doi:10.1029/2004GL021592.
- Robock, A. (2000), Volcanic eruptions and climate, *Rev. Geophys.*, *38*, 191–219.
- Russell, G. L., et al. (2000), Regional sea level changes projected by the NASA Atmosphere-Ocean Model, *Clim. Dyn.*, *16*, 789–797.
- Sato, M., et al. (1993), Stratospheric aerosol optical depths, 1850–1990, *J. Geophys. Res.*, *98*, 22,987–22,994.
- Stenchikov, G., K. Hamilton, R. J. Stouffer, A. Robock, V. Ramaswamy, B. Santer, and H.-F. Graf (2006), Arctic Oscillation response to volcanic eruptions in the IPCC AR4 climate models, *J. Geophys. Res.*, *111*, D07107, doi:10.1029/2005JD006286.
- Stott, P. A., et al. (2000), External control of twentieth century temperature by natural and anthropogenic causes, *Science*, *290*, 2133–2137.
- Weaver, A. J., et al. (2000), Evaluation of ocean and climate models using present-day observations and forcing, *Atmos. Ocean*, *38*, 271–301.
- Wigley, T. M. L., and S. C. B. Raper (2001), Interpretation of high projections for global-mean warming, *Science*, *293*, 451–454.
- Wigley, T. M. L., C. M. Ammann, B. D. Santer, and S. C. B. Raper (2005), Effect of climate sensitivity on the response to volcanic forcing, *J. Geophys. Res.*, *110*, D09107, doi:10.1029/2004JD005557.
- K. AchutaRao, P. J. Gleckler, B. D. Santer, and K. E. Taylor, Program for Climate Model Diagnosis and Intercomparison, Lawrence Livermore National Laboratory, P.O. Box 808, Livermore, CA 94551–0808, USA. (pgleckler@llnl.gov)
- J. M. Gregory, Department of Meteorology, University of Reading, Earley Gate, P.O. Box 243, Reading RG6 6BB, UK.
- T. M. L. Wigley, National Center for Atmospheric Research, 1850 Table Mesa Drive, Boulder, CO 80305, USA.